Solar Energy Materials & Solar Cells 117 (2013) 531–536

Contents lists available at ScienceDirect

Solar Energy Materials & Solar Cells

journal homepage: www.elsevier.com/locate/solmat

Improving efficiency of InGaN/GaN multiple quantum well solar cells using CdS quantum dots and distributed Bragg reflectors

Yu-Lin Tsai [a], Chien-Chung Lin [b], Hau-Vei Han [a], Chun-Kai Chang [a], Hsin-Chu Chen [a,e], Kuo-Ju Chen [a], Wei-Chi Lai [c], Jin-Kong Sheu [c], Fang-I Lai [d], Peichen Yu [a], Hao-Chung Kuo [a,*]

[a] Department of Photonics and Institute of Electro-Optical Engineering, National Chiao Tung University, Hsinchu 30010, Taiwan
[b] Institute of Photonic System, College of Photonics, National Chiao-Tung University, Tainan 71150, Taiwan
[c] Institute of Electro-Optical Science and Engineering, National Cheng Kung University, Tainan 70101, Taiwan
[d] Department of Photonics Engineering, Yuan-Ze University, Taoyuan 32070, Taiwan
[e] Electronics and Optoelectronics Research Laboratories, Industrial Technology Research Institute, Hsinchu 30010, Taiwan

ARTICLE INFO

Article history:
Received 23 January 2013
Received in revised form
11 June 2013
Accepted 2 July 2013
Available online 15 August 2013

Keywords:
InGaN multiple quantum well solar cells
Quantum dots
Luminescent down shifting
Anti-reflection

ABSTRACT

This work demonstrates hybrid InGaN/GaN multiple quantum well (MQW) solar cells with enhanced power conversion efficiency using colloidal CdS quantum dots (QDs) and back-side distributed Bragg reflectors (DBRs). CdS QDs can absorb ultraviolet (UV) photons, which are strongly absorbed by indium tin oxide (ITO), and they emit photons with a longer wavelength. This process improves the collection of photon-generated carriers and is known as the luminescence down-shifting (LDS). Accordingly, CdS QDs can compensate for the poor utilization of UV photons in an ITO layer, enhancing the external quantum efficiency (EQE) in the UV range. The DBRs on the back of the solar cells can reflect photons of longer wavelengths back into the absorber layer, increasing the EQE (380–440 nm). The combination of CdS QDs and DBRs results in broadband EQE enhancement, and yields an overall power conversion efficiency that is 20.7% better than that of a reference device without CdS QDs and DBRs.

1. Introduction

InGaN-based alloys are extensively utilized in light-emitting diodes (LEDs) and laser diodes (LDs). In recent years, InGaN-based alloys have also been considered for use in solar cells because of their favorable photovoltaic properties, including a direct bandgap, a high absorption coefficient at the band edge (of the order of 10^5 cm^{-1}), high carrier mobility, superior radiation resistance, thermal stability [1,2], and, most importantly, the wide bandgap of the InN/GaN alloy materials from 0.7 eV to 3.4 eV, which covers almost all of the solar spectrum [3,4]. Additionally, four-junction solar cells with a theoretical conversion efficiency of over 60% have been designed, but these designs require junctions that have bandgaps of greater than 2.4 eV [5]. Very few materials have a bandgap of over 2.4 eV [6], but InN/GaN alloy does. Therefore, InN/GaN alloy is a candidate for use in highly efficient tandem solar cells.

Many challenges must be overcome before InGaN-based photovoltaic devices can be used widely. A large lattice mismatch between GaN and InN limits InGaN-based photovoltaic devices to incorporate a thick absorber with a high indium content for absorbing light. Generally, the critical thickness of $In_{0.1}Ga_{0.9}N$ is approximately 100 nm, and this thickness falls rapidly as the indium content increases [7]. When the thickness of InGaN layer exceeds a critical value, defects are formed as recombination centers [8]. These recombination centers increase the rate of consumption of photo-generated electron–hole pairs, degrading photovoltaic performance. Owing to the need for high crystalline quality, the thickness of absorbers in InGaN-based photovoltaic devices is limited by challenges related to epitaxial deposition such that a compromise of multiple quantum well (MQW) structure is used for the absorbers in InGaN-based photovoltaic devices, which results in insufficient light absorption [9]. However, indium tin oxide (ITO) is typically deposited as a conducting and transparent layer, but it has a high absorption coefficient in the ultraviolet (UV) region without generating a photocurrent. Therefore, a new approach for overcoming the insufficient light absorption and reducing the high absorption of the ITO layer is needed.

Previous studies have utilized several methods for improving the harvesting of light in InGaN/GaN MQW solar cells, such as the use of a ZnO or SiO_2 sub-wavelength structure to realize a graded refractive index interface to reduce Fresnel reflection and simultaneously to increase the light scattering effect [10,11]. Silver nanoparticles have also been used to exploit the surface plasmonic effect to promote the scattering of light [12]. However, neither the

* Corresponding author. Tel.: +886 5712121x31986.
E-mail addresses: chienchunglin@faculty.nctu.edu.tw (C.-C. Lin), hckuo@faculty.nctu.edu.tw (H.-C. Kuo).

0927-0248/$ - see front matter © 2013 Elsevier B.V. All rights reserved.
http://dx.doi.org/10.1016/j.solmat.2013.07.004

problem of high absorption in the ultraviolet region by ITO layer nor that of the low external quantum efficiency (EQE) owing to the insufficient light absorption has been solved. A back reflector that reflects the unused light back to the absorber layer provides a solution and has an important role in thin-film solar cells [13]. For this purpose, distributed Bragg reflectors (DBRs) are good candidates for InGaN/GaN MQW solar cells. The advantages of DBRs include high reflectance, a controllable stop band, and a controllable central wavelength [14]. Appropriately chosen DBRs can solve the problem of a low EQE in thin-film solar cell.

In the past, quantum dots (QDs) have been extensively used in optoelectronic devices, such as LEDs and solar cells. CdS QDs on the top of solar cells with luminescent down shifting (LDS) and anti-reflective characteristic have recently been demonstrated [15–17]. The QDs with LDS effect can absorb UV light and emit light of longer wavelength, solving the problem of high absorption of UV light by the ITO layer.

This work demonstrates hybrid InGaN/GaN MQW solar cells in which colloidal CdS QDs and back-side DBRs are used to promote their harvesting of light. The characteristics of InGaN/GaN MQW solar cells with colloidal CdS QDs and back-side DBRs were determined by obtaining reflectance spectra, EQE, and a current density–voltage (*J–V*) profile.

2. Process and structure

The InGaN/GaN MQW solar cells were grown by metal–organic chemical vapor deposition (MOCVD) on a *c*-plane sapphire substrate. The devices comprised a 30 nm-thick, low-temperature GaN nucleation layer and a 2 μm-thick undoped GaN layer on sapphire substrate, 14-period $In_{0.15}Ga_{0.85}N$/GaN (3 nm/5 nm) undoped MQW sandwiched by a 2 um-thick Si-doped n-GaN layer (n-doping$=2\times10^{18}$ cm^{-3}) and a 200 nm-thick Mg-doped p-GaN layer (p-doping$=2\times10^{17}$ cm^{-3}). A 110 nm-thick indium-tin-oxide (ITO) p-GaN conducting layer was deposited by a sputtering system. The device was then defined using a 2×2 mm^2 mesa and an inductively coupled plasma reactive ion etching (ICP-RIE) system. Finally, Cr/Pt/Au (50/50/1900 nm) was deposited by electron-beam evaporation, which serves as the p-GaN and the n-GaN contact metal.

The DBRs comprised 11-period HfO_2/SiO_2, and were deposited on the glass substrate and grown by an electron beam evaporation system at room temperature. To control the central wavelength and the stop band of the DBRs, quartz was used to monitor the deposition rates. Fig. 1(a) plots the obtained reflectance spectra of 11-period HfO_2/SiO_2 DBRs from a wavelength of 385 nm to a wavelength of 460 nm, with a reflectance of over 98%.

Following regular semiconductor processes, the spin-coating method was used to form a CdS QDs thin film on the top of the device and 11-period HfO_2/SiO_2 DBRs were put on the back of device. In this study, a colloidal CdS QDs solution in toluene with a concentration of 1 mg/ml was used. Fig. 1(b) presents the device structure with CdS QDs and DBRs.

Fig. 2(a) presents the absorbance and photoluminescence spectra of CdS QDs in toluene. The absorbance spectrum includes a sharp rising edge around 400 nm and exhibits peak absorption at approximately 380 nm. The photoluminescence spectrum was obtained with 365 nm excitation, and a major emission wavelength of approximately 405 nm was found. The inset in Fig. 2(a) presents the InGaN/GaN MQW solar cells with CdS QDs not irradiated and irradiated with a UV light. Fig. 2(b) and (c) presents 45-tilted (Fig. 2b), and cross-sectional (Fig. 2c) scanning electron microscopic (SEM) images of CdS QDs on the top of InGaN/GaN MQW solar cells. The approximately nanospherical structures on the surface were the self-assembled CdS QD clusters with diameters of 80–100 nm [18]. In this study, four types of InGaN/GaN MQW solar cell are prepared for analysis—one with CdS QDs, one with DBRs, one with both CdS QDs and DBRs, and one bare cell as a reference.

The system for measuring power conversion efficiency (PEC) comprised a power supply (Newport 69920), a 1000 W Class A solar simulator (Newport 91192A) with a xenon lamp (Newport 6271A) and an Air Mass 1.5 Global (AM1.5 G) filter (Newport 81088A), and a probe stage with a source-meter (Keithley 2400). The use of the PEC measuring system closely followed the procedure in international standard CEI IEC 60904-1. The spectrum of the solar simulator was measured using a calibrated spectro-radiometer (Soma S-2440) at wavelengths in the range 300–1100 nm. The devices were operated under a 1000 W Class A solar simulator with AM1.5 G illumination [19] with a power density of 1000 W/m^2. The temperature was maintained at 25 ± 1 °C during the measurements using an automatic temperature control system. According to the calibration report by Newport Corporation, the temporal instability was 0.88%, and the non-uniformity was 0.79%. Before measurements were made, the intensity of the solar simulator was calibrated using a mono-crystalline silicon reference cell with a 2 cm × 2 cm illumination area (VLSI Standards, Inc.).[20].

The system for measuring external quantum efficiency (EQE) comprised a 300 W xenon lamp (Newport 66984) with a monochromator (Newprot 74112), a lock-in amplifier (Standard Research System, SR830), an optical chopper unit (SR540) that was operated at a chopping frequency of 260 Hz, and a 1 Ω resistor in a shunt connection to transform the photocurrent to voltage. Before measurements were made, a calibrated silicon photodetector with a known spectral response (Newport 818-UV) was used to calibrate the EQE measuring system. During the measurement process, the temperature of the probe stage was maintained at 25 ± 1 °C using an automatic temperature control system.

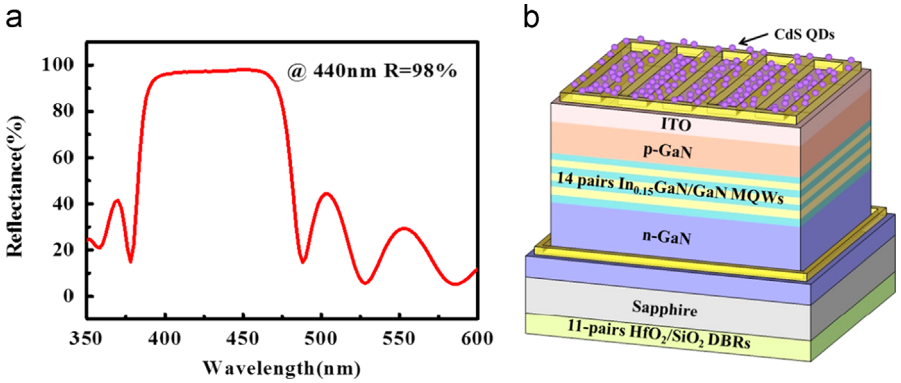

Fig. 1. (a) Measured reflectance spectra of 11-period HfO_2/SiO_2 DBR (b) Schematic illustration of InGaN/GaN MQW solar cell with CdS QDs and DBRs.

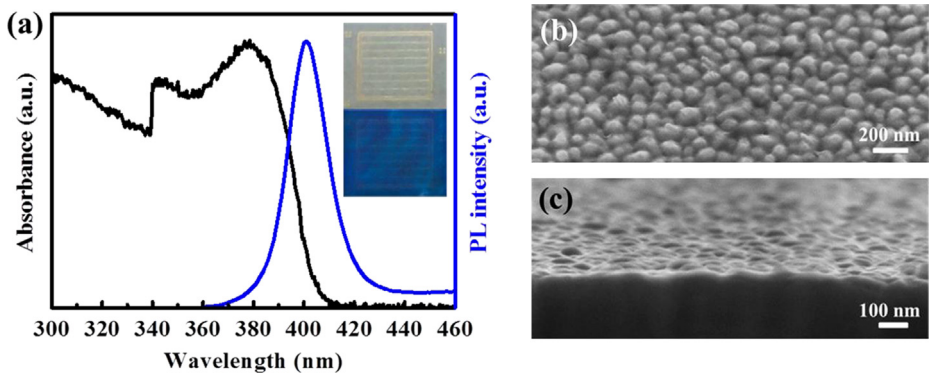

Fig. 2. (a) Measured photoluminescence (blue) and UV–vis absorbance (black) spectra of CdS QDs in toluene. Inset in (a) presents InGaN/GaN MQW solar cells with CdS QDs not irradiated and irradiated under UV light. SEM image of CdS QDs on top of InGaN/GaN MQW solar cells; (b) 45°tilted view, and (c) cross-sectional view. (For interpretation of the references to color in this figure legend, the reader is referred to the web version of this article.)

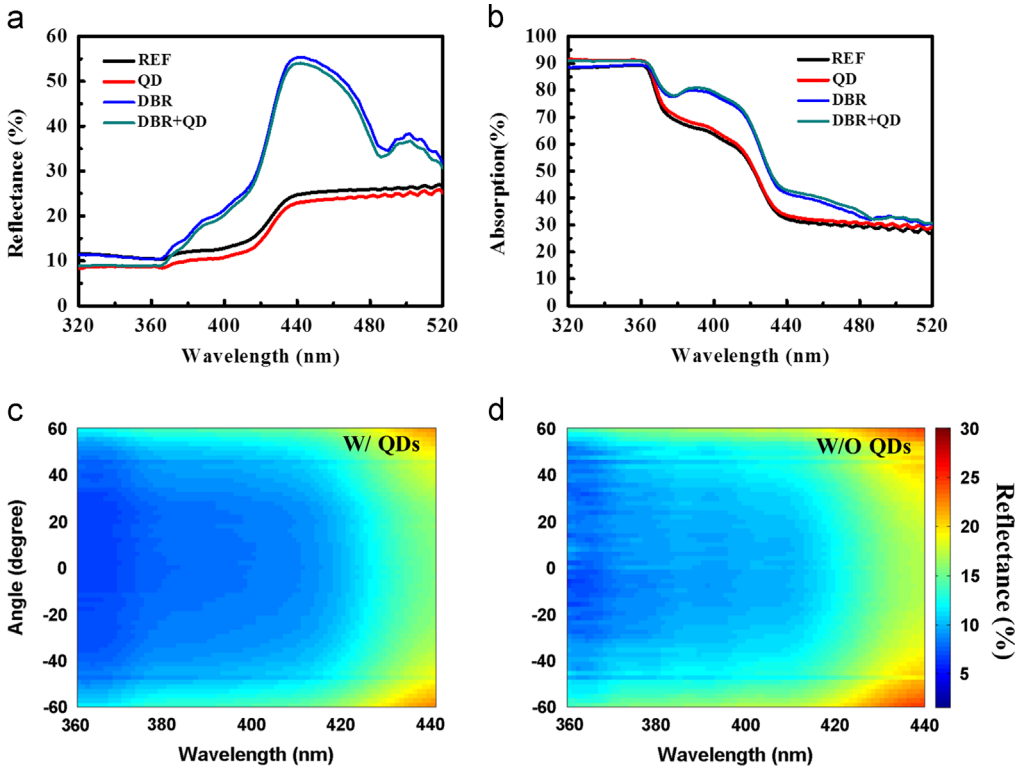

Fig. 3. (a) Measured reflectance spectra. (b) Measured absorption spectra of InGaN/GaN MQW solar cells with CdS QDs, cell with DBR, cell with both CdS QDs and DBRs, and bare cell as reference. Measured angle-resolved reflectance spectra of InGaN/GaN MQW solar cells (c) with CdS QDs (d) without CdS QDs.

3. Measurement and analysis

Fig. 3(a) and (b) presents the reflectance spectra and absorption spectra respectively of the InGaN/GaN MQW solar cells with CdS QDs, the cell with DBRs, the cell with both CdS QDs and DBRs, and the reference bare cell. A comparison of the reflectance spectra of the cell with and without QDs reveals that CdS QDs provide a significant broadband anti-reflection property. The scattering of light by the CdS QD nano-clusters is responsible for the anti-reflection characteristic of the CdS QD nano-clusters. Additionally, since the wavelengths of incident photons exceed the dimension of the CdS QD nano-clusters, according to the effective medium theory, these clusters provide an interface with a graded refractive index, resulting in a broadband anti-reflection characteristic that promotes light harvesting [21]. Fig. 3(b) presents the absorption spectrum of each device; at wavelengths below 390 nm, the cell with QDs and that with both QDs and DBRs have higher absorption than that without QDs. The improvement in absorption is attributable to both the absorption and the anti-reflective characteristic of the CdS QD nano-clusters. According to the reflectance spectra of the DBRs, the improvement of absorption of wavelengths from 390 to 440 nm is attributable to both the anti-reflectance characteristic of the CdS QD nano-clusters and the high reflectance of DBRs. Fig. 3(c) and (d) presents the measured angle-resolved reflectance of the device with and without CdS QDs, respectively. The CdS QD clusters function as an omnidirectional anti-reflective layer, which couples obliquely incident photons into an MQW absorber at angles of up to 60°.

Fig. 4(a) plots the measured photovoltaic current density–voltage (J–V) curves of the four types of InGaN/GaN MQW solar cell under simulated AM1.5 G illumination. Table 1 presents the measurements in detail. The short-circuit current density (J_{SC}) of the cell with only CdS QDs and the cell with only DBRs are 5.5% and 16.5% better than that of the reference cell, respectively.

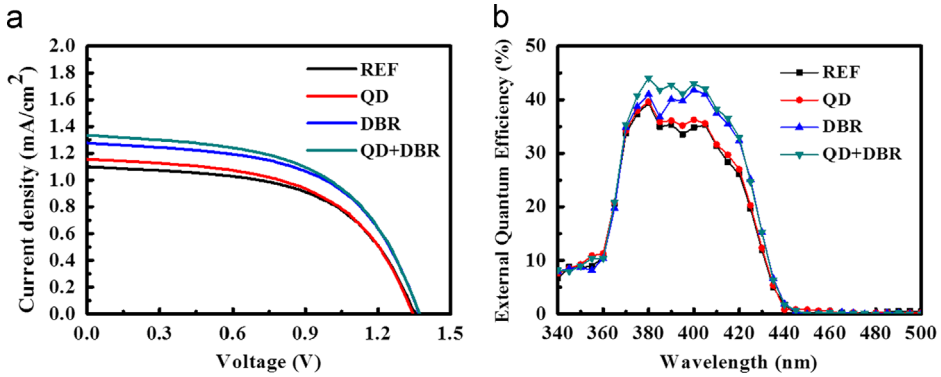

Fig. 4. (a) Measured photovoltaic current density–voltage (J–V) curve. (b) Measured external quantum efficiency (EQE) of InGaN/GaN MQW solar cell with CdS QDs, cell with DBR, cell with both CdS QDs and DBRs, and bare cell as reference.

Table 1
Current–voltage characteristics of InGaN/GaN MQW solar cells with CdS QDs, cell with DBR, cell with both CdS QDs and DBRs, and bare cell as reference.

Type	V_{oc} (V)	J_{sc} (mA/cm^2)	F.F. (%)	Efficiency (%)
Reference	1.35	1.09	56.03	0.83
QDs	1.34	1.15	54.52	0.85
DBR	1.37	1.27	56.19	0.98
QDs+DBR	1.37	1.33	54.79	1.002

The combination of CdS QDs and DBRs can further enhance J_{SC} by 22%. According to Eq. (1), increasing the J_{SC} increases the open circuit voltage (V_{OC}):.

$$V_{oc} = \frac{kT}{q}\ln\left(\frac{J_{SC}}{J_0}+1\right) \quad (1)$$

A slight drop in the fill factor (F.F.) is observed when CdS QDs are added to the cells because the sprayed CdS QDs are overspilled to the sidewall of the device. As the CdS QDs cover the unprotected sidewall, under normal sunlight, there will be photogenerated electron-hole pairs in the nano-crystal and thus widen the current leakage path as the CdS QDs now are acting like nanoscale conductors. The corresponding increase on photoconductivity under illumination was detected before [16] [22]. However, the InGaN/GaN MQW solar cells with CdS QDs also exhibit increased power conversion efficiency. The cell that combines CdS QDs and DBRs exhibit the highest power conversion efficiency which is 20.7% better than that of the reference cell.

Fig. 4(b) presents the measured EQE of the four types of InGaN/GaN MQW solar cell. The EQE results provide the relationship between light absorption and photocurrent. The low EQE at wavelengths of under 360 nm is governed by many factors, including junction depth, surface recombination, and absorption of UV photons by the ITO layer. The cell with only CdS QDs exhibits an overall EQE enhancement at wavelengths from 350 to 440 nm that is attributable to the scattering of light and anti-reflective characteristic of the CdS QD nano-clusters on the top. The results herein are highly consistent with the reflectance spectra. Notably, the EQE of the cell with CdS QDs at wavelengths from 350 to 365 nm is a significant higher than that of reference cell owing to the LDS effect of the CdS QDs. When UV photons are incident into the cell with CdS QDs on top, they are absorbed not by ITO but by CdS QDs, and then converted into photons of longer wavelengths, which can therefore penetrate the ITO layer without being absorbed, reaching the MQW absorber layer. To prevent the absorption of incident photons by the ITO layer, the degradation of EQE by the poor photon-generated carrier extraction efficiency of ITO and surface recombination in the ITO layer can be suppressed. The cell with only DBRs has a significantly enhanced EQE

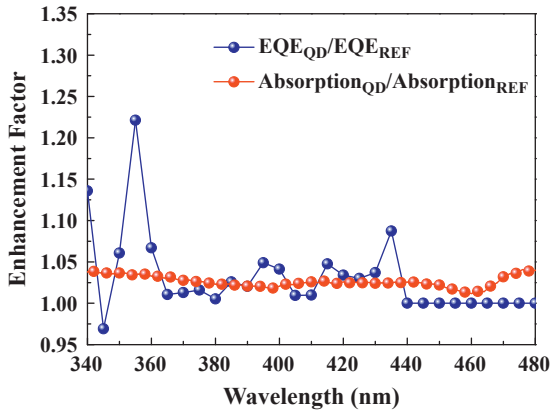

Fig. 5. Enhancement factors of EQE (blue line) and absorption (red line) of cell with CdS QDs relative to reference cell. (For interpretation of the references to color in this figure legend, the reader is referred to the web version of this article.)

at wavelengths in the range 380–440 nm because the DBRs can reflect photons back into the MQW absorber and lengthen the optical path, promoting light absorption. Combining CdS QDs with DBRs significantly enhances EQE over a broadband in the wavelength range 350–440 nm. The cell with both CdS QDs and DBRs has the highest EQE, and therefore the highest J_{SC} of the four kinds of cell.

To elucidate further the effect of CdS QDs on the InGaN/GaN MQW solar cells, their EQE and absorption are analyzed in detail below. Fig. 5 presents the enhancement factors of both the EQE and the absorption of the cell with CdS QDs relative to the reference cell. The enhancement in absorption of longer wavelengths is caused by the AR characteristic of the CdS QDs, not their LDS effect. A significant peak in EQE is observed at wavelengths in the range 350–365 nm; this peak is absent from the absorption spectrum. The difference between the enhancement in absorption spectrum and the EQE enhancement is explained with reference to the LDS of CdS QDs. Most of UV-photon-generated electron-hole pairs in solar cells are located close to the surface, which can be strongly influenced by the surface defects. CdS QDs can convert incident photons to photons of longer wavelengths, thereby reduce the effect of surface defects and the ITO layer. In Fig. 5, a large enhancement factor at wavelengths around 360 nm reveals the improvement that is provided by this CdS QD layer.

Fig. 6 presents the enhancement factors of EQE for the cell with DBRs and the cell with both QDs and DBRs relative to reference cell. The enhancement factors of EQE are calculated by EQE/EQE$_{reference}$. Both exhibit a 1.1 to 1.3-fold enhancement at wavelengths of 380–440 nm, which result is consistent with the high reflectance of DBRs. The enhancement factors of EQE of both cells

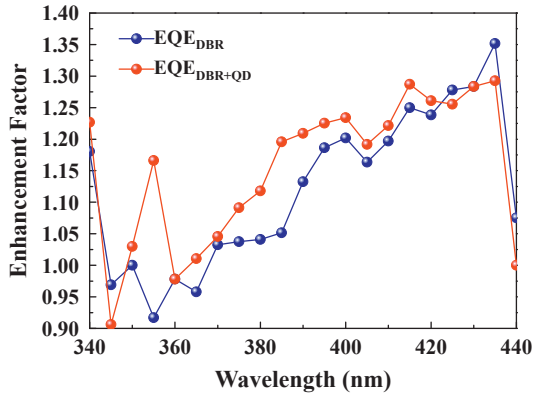

Fig. 6. Enhancement factor of EQE for cell with DBRs (blue line) and cell with both QDs and DBRs (red line) relative to reference cell. (For interpretation of the references to color in this figure legend, the reader is referred to the web version of this article.)

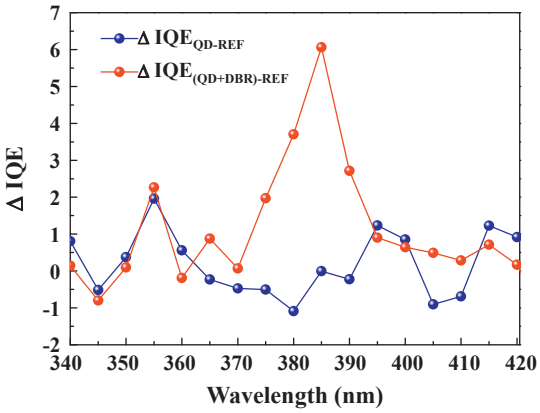

Fig. 7. The IQE difference of the cell with CdS QDs (blue line) and that of the cell with both CdS QDs and DBRs (red line) relative to reference cell. (For interpretation of the references to color in this figure legend, the reader is referred to the web version of this article.)

increase with wavelength because the absorption length depends on the wavelength of the incident photons, generally increasing with it. Restated, a photon of a longer wavelength requires a longer optical path to be absorbed. Therefore, the enhancement in EQE by DBRs is more effective at longer wavelengths. The cell with both DBRs and QDs exhibits a significant peak in the wavelength range 350–365 nm. This peak is explained by the LDS effect of CdS QDs, as stated above. Fig. 7 presents the difference between the internal quantum efficiency (ΔIQE) of the cell with DBRs and that of the cell with both DBRs and QDs. EQE differs from IQE in the efficiency of the photo-generation of carriers with or without reflection. The absorption, A, of a solar cell is calculated using Eq. (2), where R is the measured reflectance and T is the measured transmittance. EQE depends on both light absorption and photon-carrier conversion, while IQE depends only on the latter. Therefore, the variation in the light absorption among samples is eliminated by applying Eq. (3).

$$A = 1 - R - T \tag{2}$$

$$\Delta\mathrm{IQE} = (\mathrm{EQE}_{\mathrm{DBR+QD}}/A_{\mathrm{DBR+QD}}) - (\mathrm{EQE}_{\mathrm{DBR}}/A_{\mathrm{DBR}}) \tag{3}$$

The results in Fig. 7 reveal that the cell with both QDs and DBRs exhibits a remarkably increased IQE at wavelengths in the range 370–390 nm. The improvement in ΔIQE is attributable to the extra reflection by DBRs. The incorporation of DBRs causes photons to be reflected back to the CdS QDs layer and trapped in the device. Therefore, the LDS probability of CdS QDs can be increased further to increase the IQE. It can be verified that in the wavelength range 370–390 nm, the ΔIQE of the cells with only QDs is almost zero.

4. Conclusion

In conclusion, hybrid InGaN/GaN MQW solar cells that were designed with colloidal CdS QDs and back-side DBRs were demonstrated. The luminescent down-shifting (LDS) effect of CdS QDs reduces the effect of the ITO layer and the surface recombination, enhancing the EQE for light of wavelengths shorter than 365 nm. Additionally, the self-assembled CdS QD nano-clusters serve as a broadband and omnidirectional anti-reflective layer for harvesting light. The DBRs on the back of the cell effectively reflect the light back into the MQW absorber, resulting in a broadband EQE enhancement. The short circuit current densities (J_{SC}) of the cell with only CdS QDs and the cell with only DBRs are 5.5% and 16.5% better than that of the reference cell, respectively. The combination of CdS QDs and DBRs increases the J_{SC} by 22% over that of the reference cell. The cell with only CdS QDs has an overall power conversion efficiency that is 2.4% better than that of the reference cell. The combination of CdS QDs and DBRs increases the power conversion efficiency further boosted to 20.7% better than that of the reference cell. We believe that the hybrid InGaN/GaN MQW solar cells with QDs and DBRs viably provide highly efficient conversion of solar energy.

Acknowledgments

This work was supported by the National Science Council (NSC) of Taiwan under contract nos. NSC-100-3113-E-182-001-CC2 and NSC-100-2112-M-182-004. C.C.L. is grateful for the financial support of National Science Council of Taiwan under contract no. NSC99-2221-E-009-052-MY3. H.C.K and C.C.L. would also like to thank the Advanced Optoelectronic Technology Center, National Cheng Kung University for support. Ted Knoy is appreciated for his editorial assistance.

References

[1] O. Jani, I. Ferguson, C. Honsberg, S. Kurtz, Design and characterization of GaN/InGaN solar cells, Applied Physics Letters 91 (2007) 132117-1–132117-3.
[2] A. David, M.J. Grundmann, Influence of polarization fields on carrier lifetime and recombination rates in InGaN-based light-emitting diodes, Applied Physics Letters 97 (2010) 033501-1–033501-3.
[3] J. Wu, When group-III nitrides go infrared: new properties and perspectives, Journal of Applied Physics 106 (2009) 011101-1–011101-28.
[4] J. Wu, W. Walukiewicz, K.M. Yu, W. Shan, J.W. Ager III, Superior radiation resistance of $In_{1-x}Ga_xN$ alloys: full-solar-spectrum photovoltaic material system, Journal of Applied Physics 94 (2003) 6477–6482.
[5] A.G. Bhuiyan, K. Sugita, A. Hashimoto, A. Yamamoto, InGaN solar cells: present state of the art and important challenges, IEEE Journal of Photovoltaics 2 (2012) 276–293.
[6] A. Yamamoto, Md.R. Islam, T.T. Kang, A. Hashimoto, Recent advances in InN-based solar cells: status and challenges in InGaN and InAlN solar cells, Physica Status Solidi C 7 (2010) 1309–1316.
[7] A. Luque, A. Martí, Increasing the efficiency of ideal solar cells by photon induced transitions at intermediate levels, Physical Review Letters 78 (1997) 5014–5017.
[8] M. Leyer, J. Stellmach, C. Meissner, M. Pristovsek, M. Kneissl, The critical thickness of InGaN on (0 0 0 1) GaN, Journal of Crystal Growth 310 (2008) 4913–4915.
[9] E. Matioli, C. Neufeld, M. Iza, S.C. Cruz, A.A. Al-Heji, X. Chen, R.M. Farrell, S. Keller, S. DenBaars, U. Mishra, S. Nakamura, J. Speck, C. Weisbuch, High internal and external quantum efficiency InGaN/GaN solar cells, Applied Physics Letters 98 (2001) 021102-1–021102-3.
[10] J. Bai, T. Wang, S. Sakai, Influence of the quantum-well thickness on the radiative recombination of InGaN/GaN quantum well structures, Journal of Applied physics 88 (2000) 4729–4733.
[11] G.J. Lin, K.Y. Lai, C.A. Lin, Y.-L. Lai, J.H. He, Efficiency enhancement of InGaN-based multiple quantum well solar cells employing antireflective ZnO nanorod arrays, IEEE Electron Device Letters 32 (2011) 1104–1106.

[12] P.H. Fu, G.J. Lin, C.H. Ho, C.A. Lin, C.F. Kang, Y.L. Lai, K.Y. Lai, J.H. He, Efficiency enhancement of InGaN multi-quantum-well solar cells via light-harvesting SiO_2 nano-honeycombs, Applied Physics Letters 100 (2012) 013105-1–013105-4.
[13] H. Sai, M. Kondo, Light trapping effect of patterned back surface reflectors in substrate-type single and tandem junction thin-film silicon solar cells, Solar Energy Materials & Solar Cells 95 (2011) 131–133.
[14] S.J. Chang, C.F. Shen, M.H. Hsieh, C.T. Kuo, T.K. Ko, W.S. Chen, S.C. Shei, Nitride-Based LEDs With a hybrid Al mirror+TiO_2/SiO_2 DBR backside reflector, Journal of Lightwave Technology 26 (2008) 3131–3136.
[15] H.C. Chen, C.C. Lin, H.V. Han, K.J. Chen, Y.L. Tsai, Y.A. Chang, M.H. Shih, H.C. Kuo, P. Yu, Enhancement of power conversion efficiency in GaAs solar cells with dual-layer quantum dots using flexible PDMS film, Solar Energy Materials & Solar Cells 104 (2012) 92–96.
[16] C.C. Lin, H.C. Chen, Y.L. Tsai, H.V. Han, H.S. Shih, Y.A. Chang, H.C. Kuo, P. Yu, Highly efficient CdS-quantum-dot-sensitized GaAs solar cells, Optics Express 20 (2012) A319–A326.
[17] H.C. Chen, C.C. Lin, H.W. Han, Y.L. Tsai, C.H. Chang, H.W. Wang, M.A. Tsai, H. C. Kuo, P. Yu, Enhanced efficiency for c-Si solar cell with nanopillar array via quantum dots layers, Optics Express 19 (2011) A1141–A1147.
[18] J.H. Fendler, Self-assembled nanostructured materials, Chemistry of Materials 8 (1996) 1616–1624.
[19] ASTMG173-03, Standard Tables for Reference Solar Spectral Irradiances, (ASTM International, West Conshohocken, Pennsylvania, 2005).
[20] K.A. Emery, C.R. Osterwald, Solar cell calibration methods, Solar Cells **27** (1989) 445–453.
[21] Y.F. Huang, S. Chattopadhyay, Y. Jen, C.Y. Peng, T.A. Liu, Y.K. Hsu, C.L. Pan, H. C. Lo, C.H. Hsu, Y.H. Chang, C.S. Lee, K.H. Chen, L. Chyong Chen, Improved broadband and quasi-omnidirectional anti-reflection properties with biomimetic silicon nanostructures, Nature Nanotechnology 2 (2007) 770–774.
[22] C.A. Leatherdale, C.R. Kagan, N.Y. Morgan, S.A. Empedocles, M.A. Kastner, M. G. Bawendi, Photoconductivity in CdSe quantum dot solids, Physical Review B 62 (2000) 2669–2680.